A finite-temperature dynamic coupled atomistic/discrete dislocation method

2005 Modelling Simul. Mater. Sci. Eng. 13 1101

(http://iopscience.iop.org/0965-0393/13/7/007)

INSTITUTE OF PHYSICS PUBLISHING MODELLING AND SIMULATION IN MATERIALS SCIENCE AND ENGINEERING

Modelling Simul. Mater. Sci. Eng. **13** (2005) 1101–1118 doi:10.1088/0965-0393/13/7/007

A finite-temperature dynamic coupled atomistic/discrete dislocation method

S Qu[1], V Shastry[1], W A Curtin[1] and R E Miller[2]

[1] Division of Engineering, Box D, Brown University, Providence, RI 02912, USA
[2] Department of Mechanical and Aerospace Engineering, Carleton University, 1125 Colonel By Drive, Ottawa, ON K1S 5B6, Canada

Received 21 December 2004, in final form 17 August 2005
Published 12 September 2005
Online at stacks.iop.org/MSMSE/13/1101

Abstract

A method for simultaneously thermostatting an atomistic region and absorbing energetic pulses impinging on the atomistic/continuum interface from the atomistic region is developed to operate within the framework of the coupled atomistic/discrete dislocation method. The approach inserts an additional Langevin damping term and a random force term into the equations of motion for atoms in a 'stadium' boundary region near the atom/continuum interface, with the damping coefficient ramped linearly over the width of the region, as suggested by Holian and Ravelo. The remaining interior atom dynamics are computed using a standard MD algorithm with no artificial damping or thermostatting. The continuum region deformations are computed using static FEM updated stochastically over time scales comparable to the Debye frequency of the atoms using time-averaged displacements at the atom/continuum interface, thereby providing an evolution of the continuum region that tracks the atomistic deformation. The method is evaluated by studying the ability of the coupled system: (i) to equilibrate the inner atomistic region at a desired temperature under conditions of no external or internal loading, (ii) to produce the proper canonical thermal fluctuations and (iii) to absorb deformation pulses initiated in the interior region and incident upon the atomistic/continuum boundary. With an optimal maximum damping coefficient of approximately 1/2 of the Debye frequency, temperature stability is attained at values very close to the target temperature. The temperature variance agrees well with the canonical expectation for various temperatures. For the same damping parameters and at low temperature, high-energy deformation pulses propagate unimpeded up to the stadium boundary region and then are completely damped out upon approach to the atomistic/continuum interface with no measurable reflections. At higher temperatures, thermal fluctuations in the total energy make analyses difficult, but damping of high-energy deformation pulses is achieved within the limits of the thermal noise in the system while observation of the time-dependent displacements shows no observable reflections.

1. Introduction

The coupling of atomistic and continuum domains has been an active area of research in recent years. The goal of such coupling is to maintain atomistic resolution in critical regions of a material while coarse-graining the surrounding regions in a manner that preserves the elastic response of the surrounding material and avoids any artificial forces due to the interface coupling. A number of models now exist for handling static equilibrium at zero temperature; the details of these models have recently been reviewed in [1]. Dynamic models encounter additional difficulties associated with the propagation of waves across the atomistic/continuum boundary; the change in constitutive behaviour and/or the change in scale refinement can both cause spurious reflections of waves at the interface. These difficulties have been overcome at zero temperature through the use of special history-dependent boundary conditions for the atomistic problem. Such methods, about which more will be said below, have not been formally extended to finite temperatures. Finite-temperature behaviour, i.e. equilibrium thermodynamics, of coupled systems also has difficulties due to the loss of entropy in a standard coarse-graining procedure. Recent works [2, 3] have developed methods to preserve the loss of entropy through the formulation of coarse-grained potentials that depend on temperature. These approaches provide a foundation for the finite-temperature continuum thermodynamics of quasi-harmonic systems that can be coupled to a fully-atomistic region of material. The finite-temperature models do not, however, deal with the dynamic (non-equilibrium) response of the system.

As hinted above, the overarching problem in developing an accurate dynamic and finite-temperature atomistic/continuum coupling method is due to the competing physical features of dynamics and thermodynamics, i.e. non-equilibrium and equilibrium behaviour. Equilibrium thermodynamics in a canonical ensemble is usually achieved in molecular dynamics through the use of a thermostat, which artificially couples the dynamic atomistic degrees of freedom to a 'reservoir' so that the system samples the appropriate phase space over time. The thermostat adds a damping term to the equations of motion, such that the equations of motion of all the degrees of freedom are fully coupled in a non-linear manner, with a coupling constant that depends inversely on system size. One common method is the Nose–Hoover (NH) [6] thermostat that couples the entire atomistic system to a heat reservoir described by a single degree of freedom. This coupling is accomplished by modifying the atomistic equation of motion to the form [3],

$$\ddot{\boldsymbol{x}} = \frac{\boldsymbol{F}}{m} - \gamma \dot{\boldsymbol{x}}, \tag{1}$$

where $\ddot{\boldsymbol{x}}$ is the acceleration of an atom of mass m, $\dot{\boldsymbol{x}}$ is the corresponding velocity and $\boldsymbol{F}$ is the instantaneous force on the atom. γ is a damping coefficient that evolves with time as [6]:

$$\dot{\gamma} = \frac{3Nk_{\mathrm{B}}}{2Q}(T - T_0), \tag{2}$$

where k_{B} is the Boltzmann's constant, T is the instantaneous kinetic temperature of the entire system, T_0 is the desired equilibrium reservoir temperature and N is the number of atoms in the atomistic region. The parameter Q is related to the Einstein frequency ω_{E} of the crystal and is given by [3]

$$Q = ZNk_{\mathrm{B}}T_0/\omega_{\mathrm{E}}^2, \tag{3}$$

where Z is an empirical factor chosen to obtain good stability and proper canonical fluctuations in the simulation [7]. The study of dynamic problems within finite-temperature molecular

dynamics is thus feasible for large atomistic systems, where the damping of any one atom is quite small. However, a key objective in coupled atomistic/continuum models is to reduce the size of the atomistic region to a minimum, and thus a standard thermostat could strongly and improperly damp out any non-equilibrium behaviour.

An important issue for the proper study of thermally-activated phenomena in near-equilibrium systems is attainment of the proper level of fluctuations for a canonical system. For a system in the canonical ensemble, the variance of the temperature is [7]

$$\langle (\delta T)^2 \rangle_0 = \frac{2}{d} \frac{\langle T \rangle^2}{N}, \tag{4}$$

where the subscript '0' represents the canonical-ensemble value, d is the number of spatial dimensions (= 3 in the current study), $\langle \ldots \rangle$ indicates the time-averaged value and $\delta T = T - \langle T \rangle$. According to Holian *et al* [7] various common thermostats do not reach the appropriate level of fluctuations including the NH thermostat when using either an ill-chosen value of the Z parameter (weak damping) or at very low temperatures (enhanced fluctuation compared with the canonical expectation). Thus, a stable temperature is far from sufficient to ensure attainment of a canonical ensemble.

Zero-temperature dynamics in coupled systems has been considered by a number of workers [8–12]. For a material with harmonic (elastic) interactions, the interaction of one atomistic region with an adjoining atomistic region can be written exactly in terms of a history-dependent interaction term among atoms within the first atomistic region only. Such an approach eliminates the need for explicit consideration of the adjoining atomistic region. Thus, the adjoining region can be described by other methods, e.g. finite elements or other coarse-grained models, without inducing spurious reflections at the atomistic/continuum boundary because the atomistic region acts as if it is embedded in a fully atomistic problem. All of the various works to date are based on a similar underlying formalism, with different approximations or methods used to obtain an operational method. The modified equations of motion for the atomistic system can be written in the general form:

$$\ddot{\boldsymbol{x}}_i = \frac{\boldsymbol{F}_i}{m} - \sum_j^M \int_0^t \beta_{ij}(\tau) \dot{\boldsymbol{x}}_j (t - \tau)\, \mathrm{d}\tau, \tag{5}$$

where bold-face type indicates vectors and/or tensors and the indices indicate specific atoms and M is the number of atoms in the neighbourhood of atom i, including atom i. The second term in equation (5) involves a time-dependent kernel β_{ij} that couples pairs of atoms that are within r_c of each other and of the interface, where r_c is the cut-off distance of the interatomic forces. Cai *et al* [10] introduced a numerical method to calculate the β_{ij} exactly for any atomistic system. Weinan and Huang [11] introduced an approximation to the second term as well as a method for coupling the atomistic description to an overlapping coarse-grained description of the dynamics. Wagner and Liu [12] introduced a method based on projection operators to separate out fine-scale and coarse-scale deformations and vibrations, evaluated the β_{ij} exactly for a one-dimensional harmonic chain of atoms and examined the accuracy of using the elastic β_{ij} for non-linear systems. All of these approaches operate at zero temperature. There is an apparent finite-temperature-like term in the dynamics that is associated with the random initial conditions of the second atomistic region. Such a term could be used as an additional forcing term to approximate thermal fluctuations, but no formal framework for coupling of these methods to a finite-temperature reservoir has yet been achieved.

Abraham *et al* [13] formulated a coupled method using a single Hamiltonian function for the entire system that could then be used in a standard finite-temperature formulation. Although

no notable wave reflection at the coupling boundary was observed, the issue was not actually studied, and the method contained no explicit provisions to alleviate the standard problems causing reflections. Rudd and Broughton [14] use a coarse grained molecular dynamics (CGMD) approach to address finite-temperature behaviour in mixed atomistic continuum simulations. Molecular dynamics is employed in the interior region of interest while the outer region is updated dynamically using an FEM formulation, with a graded mesh. Temperature is maintained at equilibrium, but elastic wave propagation out of the atomistic region is limited to wavelengths larger than the length scale set by the outer continuum mesh size. To create an atomistic region that absorbed waves at the boundary and thus avoided spurious reflections, Holian and Ravelo [4] used an artificial damping in a boundary layer of atoms at the outer edge of the simulation cell. This 'stadium damping' concept was employed in several simulations at zero temperature, and results on one-dimensional models were claimed to absorb waves effectively. Holland and Marder [15] have employed a similar stadium damping concept based on Langevin dynamics in their work on dynamic fracture propagation but without providing any quantitative assessment of the method. Thus, to our knowledge, no work on finite-temperature systems or data on wave damping within the 'stadium damping' framework have been presented in the literature.

In an effort to simultaneously handle both dynamic wave propagation and finite-temperature dynamics within a coupled atomistic/continuum model, we develop here a method based on the 'stadium boundary conditions' proposed by Holian and Ravelo with a Langevin-type thermostat employed by Holland and Marder [15], within the framework of a coupled atomistic/continuum model [4]. The coupled model we build upon here is the coupled atomistic discrete dislocation (CADD) model of Shilkrot *et al* [5]. The CADD model permits the continuum region to deform plastically through the explicit motion of dislocation defects and also permits the transfer of defects between fully-atomistic and continuum descriptions across the atomistic/continuum boundary. We will not exploit the full features of CADD that distinguish it from all other coupled methods but instead focus here on the development of a method for the simultaneous treatment of full Hamiltonian dynamics in an atomistic region, coupling to a reservoir to maintain a constant temperature under equilibrium conditions and elimination of spurious wave reflections at the atomistic/continuum boundary.

2. Finite-temperature dynamic CADD

The quasistatic CADD model consists of an atomistic region and a continuum region coupled through atom displacements at and near the boundary region [5]. In this method, the atomistic and continuum regions are treated as separate mechanical systems that are coupled as follows. The atom positions r_{I} at the atom/continuum interface provide displacement boundary conditions U_{I} for a continuum FEM calculation of the continuum deformation, described by continuum nodal positions U_{c}. The continuum deformation field is then projected onto individual atom positions r_{P} in a 'pad' region of atoms in the continuum region adjacent to the atom/continuum interface. These pad atoms are then considered a part of the atomistic region, and the real atoms (degrees of freedom r_{A} and r_{I}) are moved according to forces generated by the real atoms and the pad atoms. An iterative conjugate gradient algorithm consisting of (i) incremental motion of the real atoms (interior and interface atoms r_{I}) and any dislocations in the continuum, (ii) updating of the continuum nodes U_{c}, (iii) adjustment of the pad atom positions r_{P} consistent with the new continuum field and (iv) new incremental motion of the atoms r_{A} and r_{I} and continuum dislocations is performed until convergence. Details associated with dislocation transfer across the atom/continuum interface, the particularly unique feature of

CADD, are not important to the present discussion [5]. The energy functional for the atomistic region can be expressed as

$$E_{\text{atom}} = \sum_{i \in \text{A,I,P}} E_i(r_{\text{A}}, r_{\text{I}}, r_{\text{P}}), \tag{6}$$

where E_i is the energy of the ith atom as determined from appropriate interatomic potentials. The energy functional for the continuum region can be expressed as

$$E_{\text{cont}} = \sum_{\mu} E_{\mu}(U_{\text{c}}, U_{\text{I}}), \tag{7}$$

where E_μ is the energy of element μ. Atom or nodal forces are obtained as the partial derivative of the appropriate energy with respect to the desired degree of freedom plus any externally applied forces. It is important to note that the pad atoms are determined by the solution of equation (7) and not by any forces that could be derived from equation (6) in which the r_{P} appear to be degrees of freedom.

To extend the above framework to a dynamic setting, it is first worthwhile to establish the goals of such a model. First, the method should reproduce full molecular dynamics at a finite temperature in the atomistic regime so as to capture thermally-activated events, dynamic phenomena such as crack growth or dislocation motion and other finite-temperature behaviour with full resolution of atomistic details. Second, any deformation waves generated by atomistic processes and propagating outwards should be transported away from the atomistic region to avoid artificial heating and thus anomalous phenomena.

We do not consider the goal of a fully dynamic continuum region as being necessary for all coupled models. For a coupled method such as CADD where discrete dislocations will exist in the continuum region, a fully dynamic FEM may not be appropriate. Motion of the dislocations in a discrete-dislocation (DD) framework is usually achieved within a quasistatic limit, i.e. the local Peach–Koehler force on a dislocation is used to determine its velocity, and the position is then incremented accordingly for a given time step [16]. Full dynamic interaction of moving dislocations with elastic waves in the continuum is not precluded but is beyond the scope of essentially all DD formulations presently in use.

More generally, the issue of proper heat flow between atomic and continuum regions is subtle. Heat flow is a diffusive process that occurs due to the scattering of propagating waves from defects, e.g. impurities or non-linearity in the material (phonon–phonon interactions). The heat carried by wave pulses in molecular dynamics should not be converted into propagating elastic waves in the continuum, since in reality such waves should eventually scatter and transition into a diffusive heat flow. In the absence of any such scattering and conversion, elastic dynamic behaviour in the continuum may actually be unphysical except for very long wavelengths.

In practical terms, use of a dynamic continuum may also lead to unnecessary computational effort. The time required to transmit loading information from some outer continuum boundaries into the atomistic region via wave propagation may be far too long a time to run the associated molecular dynamics in the atomistic regime, i.e. the entire simulation time will be spent waiting for the loading waves to arrive in the atomistic region (e.g. a wave propagating at $3000\,\text{m}\,\text{s}^{-1}$ will require 3 ns to propagate just $10\,\mu$m). This can be mitigated by certain tricks such as sub-cycling, but it is probably preferable to avoid the problem entirely.

To accomplish the main goals above, the method here combines a *fully dynamic* atomistic region with a *quasistatic* continuum region (figure 1) for providing finite temperature and dynamics in the atomistic region while extracting appropriate energy (deformation waves) from the atomistic region when that energy would naturally propagate into, and eventually

equilibrate in, the continuum region. The following discussion deals first with the dynamics of the atomistic region and then with the quasistatic dynamics of the continuum region.

2.1. Atomistic dynamics

To thermostat the atoms and simultaneously absorb waves effectively and efficiently, a Langevin-type thermostat based on the fluctuation–dissipation thermostat is used [15, 17]. Here, a strip of atoms in the atomistic region (figure 1) that includes the atom/continuum interface atoms are given random forces and are artificially damped at each time step so that the equation of motion for an atom is

$$\ddot{\boldsymbol{x}} = \frac{\boldsymbol{F}}{m} - \gamma \dot{\boldsymbol{x}} + \chi \frac{\boldsymbol{F}_{\mathrm{A}}}{m}. \tag{8}$$

Here, γ is the applied damping and χ is a random number, $-1 \leqslant \chi \leqslant 1$. For each dimension, the component of the random force $\boldsymbol{F}_{\mathrm{A}}$ is

$$F_{\mathrm{A}i} = \sqrt{\frac{6\gamma m k T_0}{\Delta t}}, \qquad i = x, y, z, \tag{9}$$

where Δt is the size of the time step used in a discrete incremental solution to equation (8). Furthermore, the applied damping γ is a function of position relative to the atomistic/continuum interface, decreasing linearly with increasing distance from the interface as

$$\gamma = \gamma_0 \left[1 - \frac{d(x, y)}{w} \right], \tag{10}$$

where γ_0 is the maximum damping of $\sim 1/2$ of the Debye frequency, w is the width of the damped 'stadium' region and d is the minimum distance from the atom at position (x, y) to the atom/continuum boundary,

$$d(x, y) = \mathrm{abs}(\min(x - x_{\min}, x - x_{\max}, y - y_{\min}, y - y_{\max})). \tag{11}$$

Thus, the damping coefficient varies linearly from zero at a distance w inside the boundary to a value γ_0 at the boundary. This ramping permits incident waves having a wide range of wavelengths to enter the damped region and slowly be absorbed as they traverse the stadium. An abrupt change from undamped to damped atoms would create a dynamic mismatch that causes reflections and is simply unsuitable.

The stadium boundary conditions bear some resemblance, and some notable differences, to the absorbing boundary conditions characterized by equation (5). The methods are similar in that the atoms are damped in a region near the boundary with the continuum, with decreased damping as the distance to the boundary increases. The dynamics inside this region are completely independent of the boundaries and in this sense are the 'true' dynamics of the atomistic region. In the absorbing boundary condition methods, the width of the region is approximately the range of the forces, typically $\sim$10 Å for EAM-type potentials, and we will use a somewhat larger width of 20 Å below. One important difference in the methods is that the stadium approach eliminates the history-dependent coupling to surrounding neighbours in favour of a completely local and instantaneous atom damping. Formally, the stadium damping thus loses the exact nature of the time-dependent coupling. Computationally, it simplifies the problem considerably by removing the necessity of storing atom velocities in all time steps, computing damping coefficients as a weighted sum over an entire neighbourhood around each atom and performing a convolution integral. Another major difference is that the damping

here is explicitly associated with a thermal bath that represents the interaction of the stadium region with the thermal fluctuations in the surrounding (continuum) region. The damped atoms exchange kinetic energy with the interior atoms so that a non-zero equilibrium temperature can be maintained within this one framework. Lastly, no assumptions are made in the present method regarding the harmonicity or range of the interatomic interactions, so that the damping behaviour may be suitable for scenarios where atomic displacements are large and outside the linear range.

2.2. Continuum 'dynamics'

Similar to the quasistatic CADD model, we employ a quasistatic FEM to obtain the continuum fields in the coupled problem. However, since the continuum region is directly coupled to the dynamic atoms at the boundary, where the positions $r_{\mathrm{I}}(t)$ vary on the sub-picosecond time scale, we must ensure that thermal fluctuations at the boundary are not improperly propagated into the continuum as apparent permanent deformations. At the same time the continuum region should deform as the atomistic region deforms, which may occur over relatively short time scales, particularly at the high loading rates typical of an MD simulation. We thus perform the FEM calculation as follows.

First, the continuum region is characterized by the elastic constants and lattice constants (mass density) of the material at the desired equilibrium temperature, i.e. the constitutive inputs are $C_{ijkl}(T_0)$ and $a(T_0)$, as obtained from a separate MD calculation on a sample of the material of interest using the potentials employed in the atomistic region of material. Thus, the continuum material has a representation that is fully consistent with the underlying finite-temperature atomistic material; the method does not attempt to calculate the thermo-mechanical properties of the material based on only the potentials and temperature, which is a difficult task [3].

Second, the continuum fields are updated on a time scale corresponding to the typical atomic vibration frequency, which is somewhat longer than the underlying MD time scale. Specifically, the continuum fields are calculated at time increments of $\Delta t = \alpha 2\pi/\omega_{\mathrm{D}}$, where $2\pi/\omega_{\mathrm{D}}$ is the typical atom vibration period corresponding to the Debye frequency ω_{D}. The parameter α can be chosen as a fixed value or chosen stochastically within some range; we have investigated $\alpha = 0.33;\ 0.33\text{–}1.5;\ 4$ to decide the best value for thermostatting and pulse damping. Updating stochastically can avoid driving any resonance behaviour between the continuum and atomistic regions that could erroneously pump energy into, or extract energy out of, the atomistic region. If the FEM is updated too slowly, at $\Delta t \gg 2\pi/\omega_{\mathrm{D}}$, then very rapid atomistic events such as sharp wave fronts emitted during spurts of crack propagation, dislocation emission, or other events in the atomistic region, will be 'missed' by the continuum, and the system will appear to have a rigid boundary during the duration of the short event, which can enhance spurious reflections.

Third, the continuum is updated using the *time-averaged* interface displacements $\bar{U}_{\mathrm{I}} = (1/\Delta t)\int_t^{t+\Delta t} U_{\mathrm{I}}(t')\,\mathrm{d}t'$ at the interface rather than any instantaneous value. The energy functional for the continuum is then

$$E_{\mathrm{cont}} = \sum_{\mu} E_{\mu}(U_{\mathrm{c}}, \bar{U}_{\mathrm{I}}), \tag{12}$$

so that there is some averaging of the atom thermal motions before the continuum is updated. Coupled with St Venant's principle, wherein spatial fluctuations of the boundary conditions around some smooth average will die off with distance into the specimen, the effects of atomic thermal fluctuations on the continuum are minimized.

3. Testing and results

We test the ability of the method to (i) maintain a desired equilibrium temperature; (ii) achieve canonical thermal fluctuation and (iii) absorb waves impinging on the boundary from the atomistic region. We use a simple geometry consisting of a square atomistic region embedded within a larger square of continuum material. The through-thickness (z direction) is periodic using the minimum periodic distance for the crystal orientation selected. The inner atomistic region used here varies in size from 150 Å × 150 Å to 400 Å × 400 Å, as discussed below, while the overall sample size is 1000 Å × 1000 Å. Larger overall sizes are quite feasible, since the outer region is treated by the continuum method, but are unnecessary for our demonstration purposes here. The outer boundary of the sample is held at a fixed zero displacement, and no internal or external forces are applied. We use fcc aluminium as described by an EAM potential due to Ercolessi and Adams [18] having a zero-temperature cubic lattice constant $a_0 = 4.032$ Å with a crystal orientation in which the x, y and z axes all lie along [100] directions. We obtain the temperature-dependent elastic constants and lattice parameter through a separate MD calculation using DYNAMO, although the effect of this temperature dependence is small. An important material parameter for thermodynamics and dynamics is the Debye frequency $\omega_D \approx 5.6 \times 10^{13}\ s^{-1}$ for aluminium with the Debye temperature 426 K.

In general, a desired temperature T_0 is specified. The initial conditions for the atoms are zero displacement and random velocity components v_x, v_y and v_z of magnitude corresponding to $\sqrt{2}$ times the thermal velocity $\sqrt{2k_B T_0/m}$, so that the system initially contains the proper total energy for an equilibrium harmonic system at the desired temperature. The velocity Verlet algorithm is used to update the atom positions, velocities and accelerations with a time step of 1×10^{-15} s [19]. Under equilibrium conditions, after an initial transient the system attains steady state with the appropriate equipartition of kinetic and potential energies.

There are several parameters associated with the proposed stadium method: the width w of the stadium region, the maximum damping parameter γ_0 and the frequency of updating the finite elements. We cannot present the results of our extensive studies over the full range of parameters. Rather, we present results for $\gamma_0 \approx 0.45\omega_D$ with a fixed stadium width of $w = 20$ Å and FEM updating performed every 50 time steps, i.e. $\alpha \sim 0.45$ or every 5×10^{-14} s. It is observed that a smaller γ_0 (i.e. weak damping) fails to obtain canonical temperature fluctuations, similar to observations made for the NH thermostat [7]. A narrower stadium width leads to poorer damping of pulses due to a narrower range of frequencies absorbed in the stadium 'filter'. We also checked other choices of FEM updating time and found that the current one is the best for both thermostatting and pulse damping.

3.1. Thermostatting

We first present results on temperature stability and temperature fluctuations at various desired temperatures under equilibrium conditions. We use an atomistic system size of 150 Å × 150 Å which contains 5473 atoms, 2518 of which are in the stadium region (figure 1). The system is then evolved for over 10 ps and the temperature of the *undamped* atomistic region, $T = (1/3N)\sum_{i=i}^{N} m(v_x^2 + v_y^2 + v_z^2)$ (with $N = 2955$ the number of atoms in the undamped region of dimensions 110 Å × 110 Å), is monitored. In all cases, the temperature in the stadium region is stable at T_0, within the expected range of thermal fluctuations, and thus serves as an effective constant-temperature reservoir. Figure 2 shows the normalized temperature T/T_0 in the atomistic region versus the normalized time $\omega_D t$ for temperatures ranging from 1 to 300 K. The temperature stabilizes after a brief initial transient period reaching a steady value very

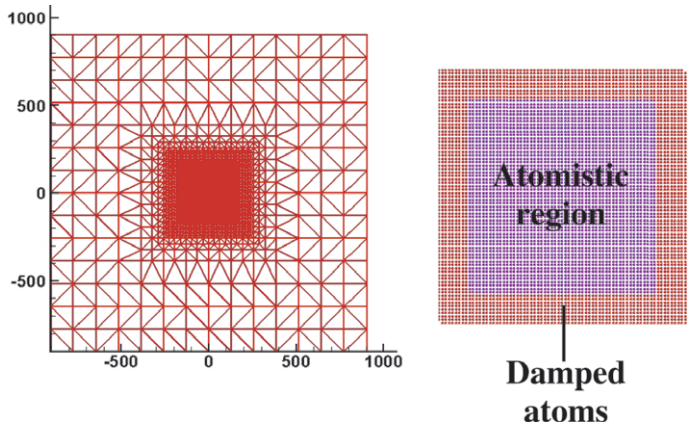

Figure 1. Schematic of the finite-temperature dynamic coupled atomistic/continuum simulation cell for the simple geometry used here showing the outer continuum FEM region, the damped stadium region of atoms near the atom/continuum boundary and an undamped atomistic region in the interior.

(This figure is in colour only in the electronic version)

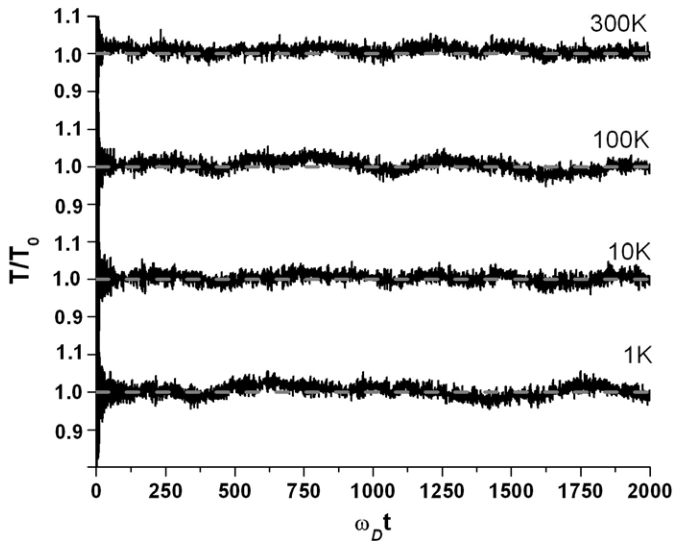

Figure 2. Normalized temperature T/T_0 in the undamped 110 Å × 110 Å region versus time for various temperature with $\gamma_0 = 0.25 \times 10^{14}\ \mathrm{s}^{-1}$, for small (150 Å × 150 Å) atomistic system sizes. Grey dashed lines indicate the desired temperature ($T/T_0 = 1$).

close to the desired temperature, as also shown in table 1. Similar stability is attained for other values of the FEM updating time, i.e. variations in the parameter α. At 300 K, we have also analysed the velocity distribution of the atoms in the system at various instants of time and verified that the distribution has the proper Maxwell–Boltzmann form.

We have also carefully studied the temperature fluctuations in the atomistic region. The variance of temperature in the system accumulated over the time span $\omega_{\mathrm{D}}t = 500$–$2000$ is shown in table 1 and agrees well with the canonical expectation at all temperatures investigated. As the system size becomes larger, the difference between $\langle(\delta T)^2\rangle_0$ and $\langle(\delta T)^2\rangle$ decreases

Table 1. Temperature and its variance for various desired temperatures T_0. The average simulated temperature is $\langle T\rangle$, $\langle(\delta T)^2\rangle_0$ is the expected canonical temperature variance (equation (4)) and $\langle(\delta T)^2\rangle$ is the variance obtained from time-averaging the simulation, where $\delta T = T - \langle T\rangle$.

Temperature (K)	$\langle T\rangle$	$\langle\delta T^2\rangle_0$	$\langle\delta T^2\rangle$	$\langle\delta T^2\rangle/\langle\delta T^2\rangle_0$
1	1.0037	1.2272e-4	1.3626e-4	1.1103
10	10.0388	0.0123	0.0108	0.8836
100	100.3543	1.2267	1.4089	1.1485
300	301.8520	11.0987	9.3942	0.8424

further. We have also verified that the stable temperature and its variance are essentially independent of the number of layers of atoms in the through-thickness z-direction. As expected, for a thickness of just one periodic distance, atoms see images of themselves which leads to correlated dynamics and a modified phonon spectrum, but this does not significantly influence the temperature variance. In light of the accurate temperature variance at low temperatures $T \ll T_D$, the present stadium damping thermostat may actually perform better than the NH thermostat in equilibrium applications over a wide temperature range.

3.2. Damping of non-equilibrium pulses

We now test the ability of the system to damp out pulses initiated in the atomistic region. In practice, such pulses might arise from spurts of crack growth, dislocation emission, frictional heating, melting or amorphization, but here artificial pulses are introduced as follows. After the system is thermally equilibrated as described above, a displacement pulse is applied at the centre of the simulation cell [12]. Specifically, we apply a radially-varying Gaussian displacement δr to each atom as a function of the distance from the centre of the simulation cell given by

$$\delta r = \frac{A}{A - u_c}(A\mathrm{e}^{-(r/\sigma)^2} - u_c) \qquad r \leqslant r_c. \tag{13}$$

A is the maximum amplitude of the pulse, usually $\sim$1 Å and σ is the pulse width, typically of the order of several angstroms. The radial displacement of all atoms located at a distance greater than r_c from the centre of the pulse is unchanged. The parameter u_c is given by

$$u_c = A\mathrm{e}^{-(r_c/\sigma)^2} \tag{14}$$

and ensures a smooth transition in the displacement at r_c. This pulse shape permits introduction of a pulse with a characteristic spectrum of wavelengths governed by σ and an amplitude that can induce non-linear response of the atomic system.

We have studied a range of parameters, but here we present results only for a 'sharp' pulse with a characteristic width equal to the nearest neighbour spacing, $\sigma = a_0/\sqrt{2}$, and for a 'broad' pulse, with $\sigma = 5a_0/\sqrt{2}$. For both cases, we show results for an amplitude of $A = 0.86$ Å that is sufficiently large for the response to be in the non-linear regime of the potential. The increase in total system potential energy upon introduction of the pulse is $\sim$5 eV for the sharp pulse and $\sim$10 eV for the broad pulse. The damping at the boundary for these pulses is presented for systems at various temperatures for the damping parameter $\gamma_0 = 0.25 \times 10^{14}\,\mathrm{s}^{-1}$ shown above for providing good overall thermostatting.

To quantitatively assess the damping requires comparison to a reference calculation in which there is no atom/continuum boundary or in which the boundary does not influence the results. We accomplish this here by comparing the damping of the 'small' sized system (atomistic region 150 Å $\times$ 150 Å, undamped in the central 110 Å $\times$ 110 Å region) to that of the

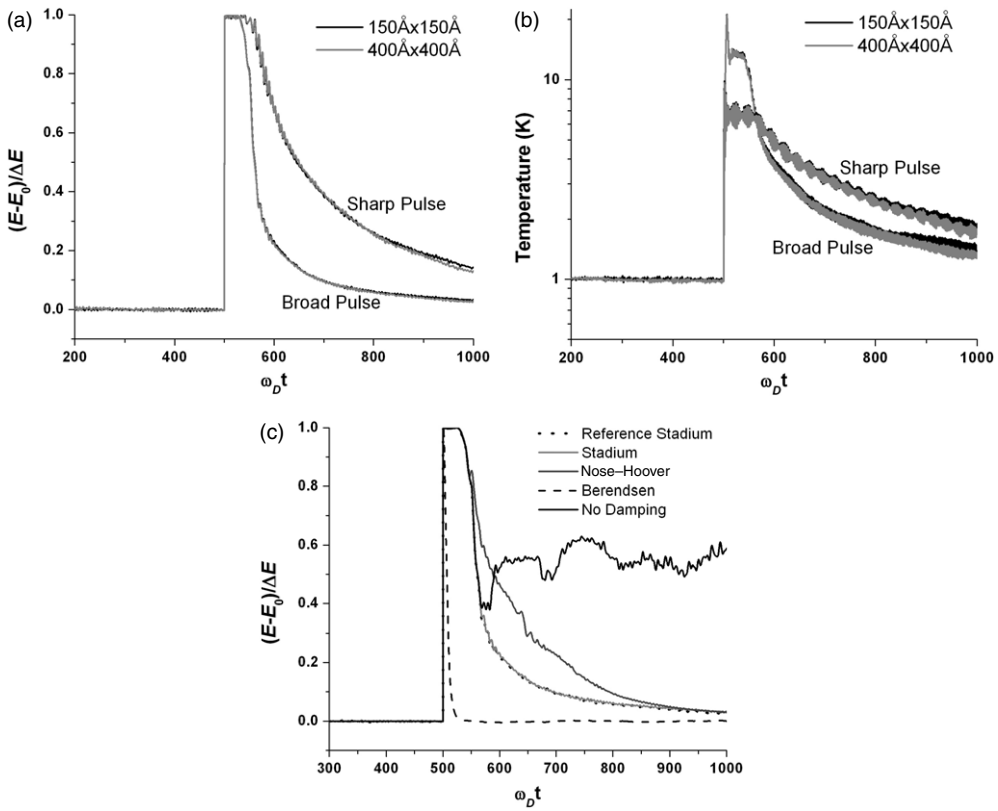

Figure 3. (*a*) Energy in the undamped 110 Å × 110 Å atomistic region versus time, with introduction of a displacement pulse, for sharp and broad pulses at 1 K for both small (150 Å × 150 Å, black) and large (400 Å × 400 Å, grey) atomistic sizes. The differences between large and small sizes can barely be discerned for either pulse width. (*b*) Temperature in the undamped 110 Å × 110 Å atomistic region versus time, with introduction of a displacement pulse, for sharp and broad pulses at 1 K for both small (black) and large (grey) atomistic sizes. (*c*) Energy in the inner 110 Å × 110 Å atomistic region versus time, with introduction of a broad displacement pulse at 1K, using (i) stadium thermostat (as in figure 3(*a*)); (ii) NH thermostat in the entire atomistic region; (iii) Berendsen thermostat in the entire atomistic region and (iv) no damping or thermostat after introduction of the pulse. Also shown is the large-system 'reference' calculation against which all results should be compared; only the stadium boundary condition adequately reproduces the reference results over the entire time domain.

'large' system (400 Å × 400 Å, undamped in the central 360 Å × 360 Å region). During the period of time in which the pulses are being damped in the small system, the pulse deformations have not reached the damped region of the larger problem. In fact, the large system is effectively infinite for times up to the time required for the pulse to travel out to the boundary at 200 Å and, if there were any reflections, travel back into the inner region within 55 Å from the centre of the simulation cell.

Figure 3(*a*) shows the total energy of the central undamped region (110 Å × 110 Å) of both small and large systems versus normalized time $\omega_{\mathrm{D}}t$ after introduction of sharp and broad pulses at 1 K, while figure 3(*b*) shows the corresponding temperatures. In this study, the total energy E is normalized by $(E - E_0)/\Delta E$, where E_0 is the steady state value of E over a long time run and ΔE is the energy jump due to the introduction of pulses. When the pulse is introduced, the energy and temperature increase very sharply and remain essentially constant

for a short period as the wave propagates through the undamped region. As energy in the pulse exits the 110 Å × 110 Å region, the remaining energy and corresponding temperature drop off smoothly. Most notably, the difference between small and large systems is completely negligible and not visible on the scale of the graphs. At this very low temperature, there is no competing thermal noise to obscure the damping behaviour. Similar behaviour is observed for other amplitudes and pulse widths. These results demonstrate that the basic stadium damping scheme coupled to a quasistatic continuum is very capable of damping out energetic pulse with negligible reflection back into the undamped region of the material. Keeping in mind that this system is thermostatted and that the pulse induces non-linear deformations in the system, these results indicating no wave reflection are quite comparable to the results found for similar studies using the zero-temperature absorbing boundary condition models [12]. We do not expect, nor demand, that the present model perform as well as the ABC models at 0 K and for perfectly linear materials but rather aim for a method that is sufficiently accurate under conditions where the ABC models also show deviations (non-linear systems) or do not yet exist (finite temperatures).

For comparison, we have studied pulse damping in the same system but using a Berendsen thermostat [20] and an NH thermostat ($Z = 1.5$ in equation (3)) over the entire atomistic region. The energy in the inner 110 Å × 110 Å region versus time is shown in figure 3(*c*), along with the stadium results from above. The Berendsen thermostat, similarly to a Hoover thermostat, immediately damps out the pulse very strongly due to the rapid rise in temperature, and the pulse does not propagate at all. The NH thermostat begins damping upon initiation of the pulse, but the time delay in effective damping prevents the pulse from being absorbed prior to reaching the atom/continuum boundary. The pulse is then reflected back into the inner 110 Å × 110 Å region and is eventually damped out after further reflections. In neither case is the system response similar to the true response of the 400 Å × 400 Å system. For further comparison, figure 3(*c*) also shows the response of a microcanonical system where, after equilibration with the thermostat, the thermostat and FEM are both eliminated upon the introduction of the pulse. The pulse thus propagates outwards, reflects off the fixed atom/continuum boundary and then undergoes multiple reflections. The times at which the dominant reflected wave enters and exits the inner region are clear, and at long times the fraction of energy in the inner region approaches the expected value $2955/5473 = 0.54$.

When the temperature is raised, thermal fluctuations begin to make comparisons between difference systems much less quantitative. In the stadium method, the thermal fluctuations in the undamped region are entirely due to the transfer of energy from the stadium reservoir. In thermal equilibrium, natural energy fluctuations in a classical system scale with the heat capacity as $\langle \delta E^2 \rangle^{1/2} \approx \sqrt{3N} k_B T_0$. The total energy fluctuations in 2900+ atoms in the 110 Å × 110 Å region at a system temperature of $T_0 = 10$ K are thus ∼0.08 eV and for $T_0 = 300$ K are ∼2.44 eV. Figures 4(*a*) and (*b*) show the energy and temperature versus time, respectively, after the introduction of a sharp and broad pulse at 10 K, in the small and large systems, and the agreement is generally good. The small system extracts energy slightly faster at intermediate times for the sharp pulse but does not show any sharp reflection. Due to the thermal noise, the agreement cannot be confirmed to the same high degree as found at the low temperature. The corresponding temperature plots show that the temperature decays similarly to the energy, as expected because the system thermalizes locally quite quickly so that the energy and temperature are closely related, since equipartition for a harmonic system implies $E = 3NkT$.

Figures 5(*a*) and (*b*) show the energy and temperature versus time, respectively, for sharp and broad pulses at 100 K, in the small and large systems. With a factor of 10 increase in temperature comes a factor of $\sqrt{10}$ increase in energy fluctuations that cloud the behaviour of

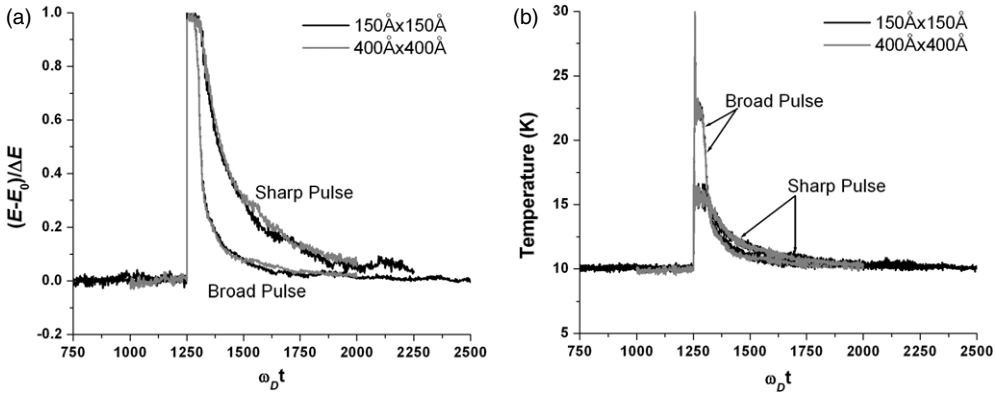

Figure 4. (*a*) Energy in the undamped 110 Å × 110 Å atomistic region versus time, with introduction of a displacement pulse, for sharp and broad pulses at 10 K for both small (black) and large (grey) atomistic sizes. (*b*) Temperature in the undamped 110 Å × 110 Å atomistic region versus time, with introduction of a displacement pulse, for sharp and broad pulses at 10 K for both small (black) and large (grey) atomistic sizes.

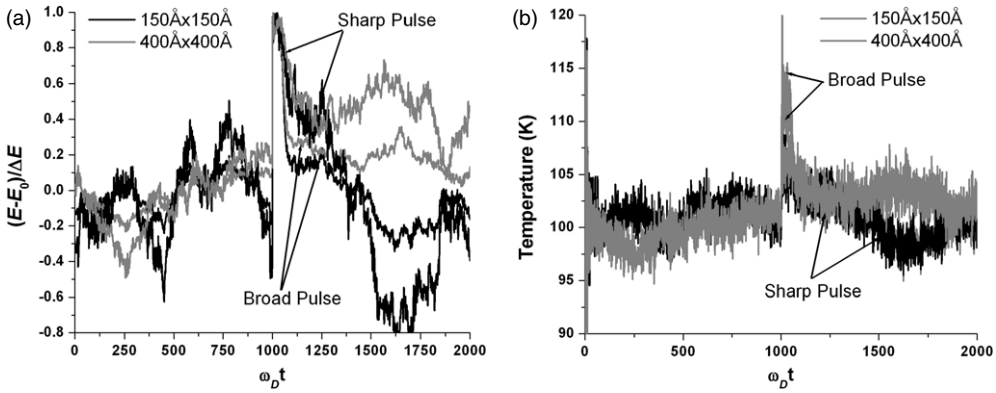

Figure 5. (*a*) Energy in the undamped 110 Å × 110 Å atomistic region versus time, with introduction of a displacement pulse, for sharp and broad pulses at 100 K for both small (black) and large (grey) atomistic sizes. (*b*) Temperature in the undamped 110 Å × 110 Å atomistic region versus time, with introduction of a displacement pulse, for sharp and broad pulses at 100 K for both small (black) and large (grey) atomistic sizes.

interest, but the small system behaviour clearly follows that of the large system during the short time over which most of the damping is accomplished, after which the thermal fluctuations render comparisons impossible. To eliminate some of the large fluctuation effects, we have performed a number of nominally identical simulations at 300 K and averaged the results of the energy and temperature versus time, respectively, leading to the results shown in figures 6(*a*) and (*b*) for the broad pulse at 300 K in the small and large systems. The agreement is again good, to within the considerable noise of the data.

To further establish that there are no notable reflections at elevated temperatures, we turn to the direct observation of the deformation histories. Figure 7 shows a sequence of contour plots of the atomic displacements at various times after introduction of the broad pulse at 100 K in both the small and large systems. At the earliest times (figures 7(*a*) and (*b*)), the pulse remains within the undamped 110 Å × 110 Å region and the deformation contours are

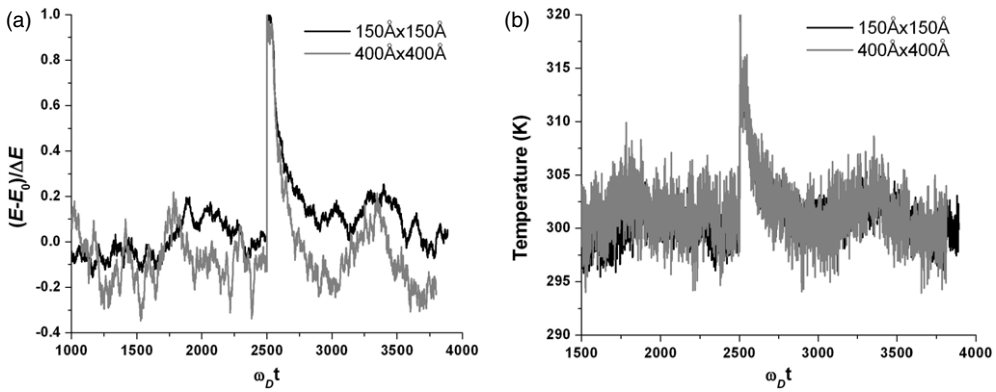

Figure 6. (*a*) Energy in the undamped 110 Å × 110 Å atomistic region versus time, with introduction of a broad displacement pulse at 300 K, for both small (black) and large (grey) atomistic sizes. Results are averages of ten individual runs for each size. (*b*) Temperature in the undamped 110 Å × 110 Å atomistic region versus time, with introduction of a displacement pulse, for the broad pulses at 300 K for both small (black) and large (grey) atomistic sizes. Results are averages of ten individual runs for each size.

very similar (aside from thermal noise). At later times as the pulse enters the stadium region of the small cell, the deformation in the 110 Å × 110 Å undamped region remains similar between the small and large simulations, but the deformation in the region of the stadium is different as the stadium successfully damps out the incident waves. At yet later times, the damping process continues, and there are no indications of any reflected waves propagating back into the undamped region. Eventually, the incident wave is completely damped (small) or propagated (large) out of the 150 Å × 150 Å field of view, and the two systems return to thermal equilibrium; figure 7(*h*) shows the typical differences that persist purely as a result of thermal fluctuations. These fluctuations account for most differences between the two simulations evident in figures 7(*a*)–(*g*).

4. Discussion and conclusions

We have shown that the stadium damping method with a Langevin-type thermostat implemented within a coupled atomistic/continuum model can serve as a thermal reservoir to maintain a stable temperature and produce canonical thermal fluctuation and also serve as an effective absorbing boundary to prevent artificial reflections and overheating of the atomistic regime. Both features can be accomplished with a ramped damping parameter having a maximum damping coefficient of ∼1/2 of the Debye frequency over a spatial range of 20 Å. We discuss below some further issues and considerations regarding thermostatting and damping in coupled systems.

The damping employed here is spatially localized to the atoms. The thermostat does not couple a large atomistic region through a global thermostat, as typically done [6, 7, 20]. Thus, the damping observed here, such as shown in figure 7, is occurring quite independently in different regions of the stadium. We use fairly energetic pulses to overcome thermal noise and to test non-linear response, but the locality of the damping indicates that large local displacements, such as those emanating from a propagating dislocation, should be damped comparably to the pulses observed here. In other words, any local disturbance reaching the boundary in some small region should be damped properly. This has been confirmed by studying pulses introduced away from the centre of the simulation cell.

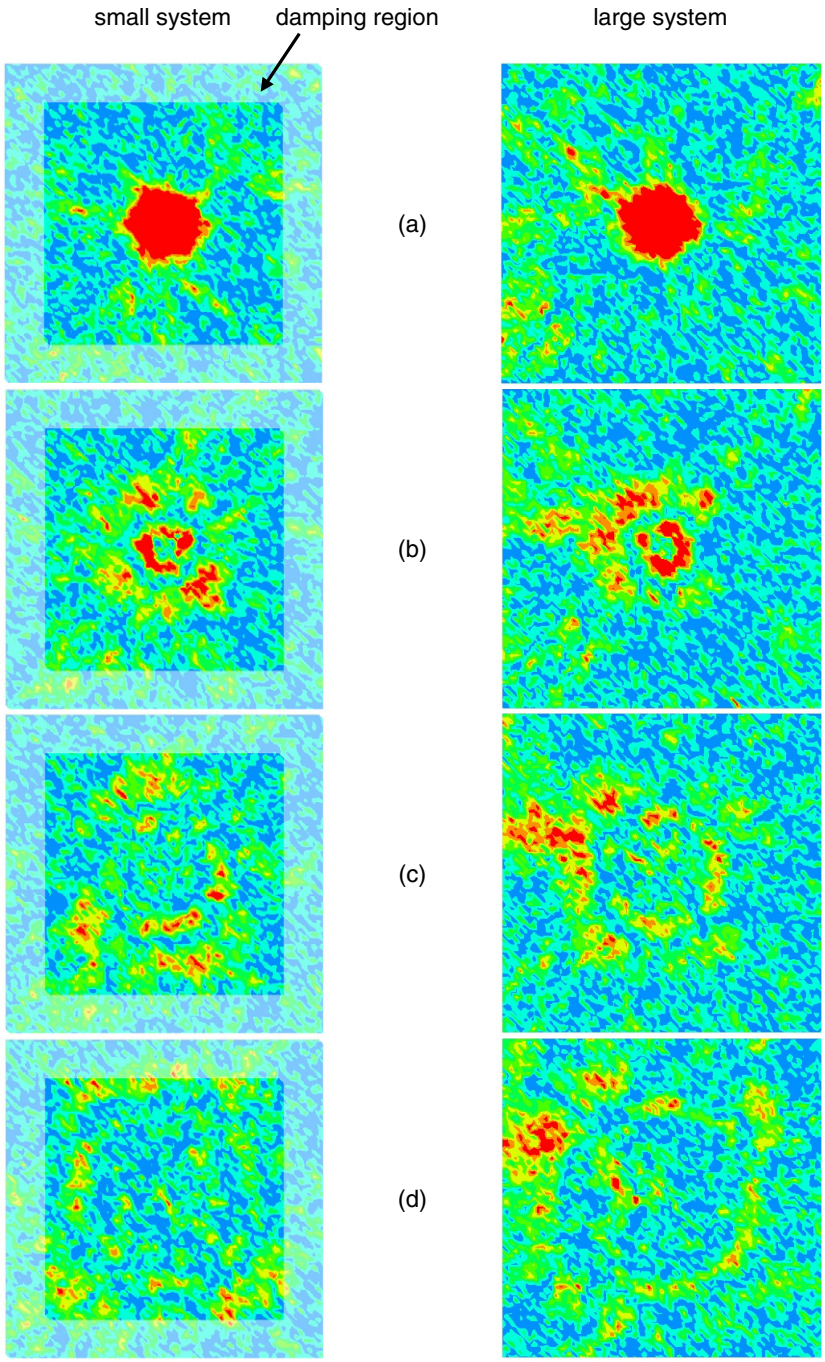

Figure 7. Snapshots of pulse displacement fields for a broad pulse at 100 K in the 150 Å × 150 Å region of both small (left side; atomistic size 150 Å × 150 Å) and large (right side; atomistic size 400 Å × 400 Å) after introduction of the pulse, corresponding to energy data in figure 5(*a*): (*a*) $\omega_{\mathrm{D}}t = 0$, (*b*) $\omega_{\mathrm{D}}t = 14$, (*c*) 28, (*d*) 42, (*e*) 56, (*f*) 70, (*g*) 84 and (*h*) 840 (thermal equilibrium). The shaded region for the small system size indicates the stadium region of damped atoms; comparisons between large and small should thus be evaluated only in the inner region (110 Å × 110 Å) of each pair of figures. Red corresponds to displacements larger than 0.25 Å; colour scale indicates displacement in Angstrom.

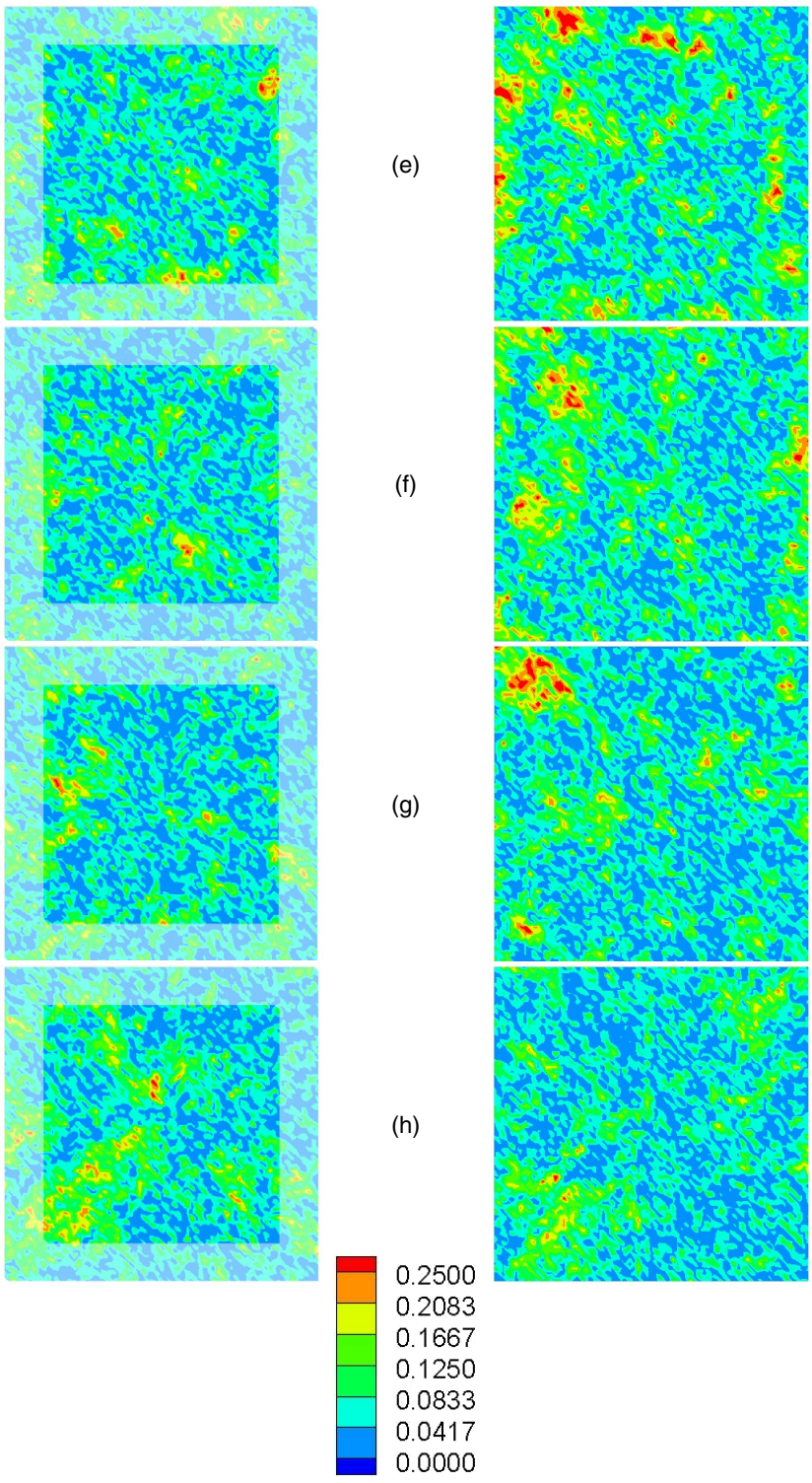

Figure 7. (Continued.)

Various modifications to the thermostatting of the atomistic domain were studied. An NH thermostat in the total atomistic region was used, leading to satisfactory temperature stability but poor damping, especially at 1 K (see figure 3(*c*)). Of course, pulses were eventually damped out since the thermostat drives the system back to equilibrium at the desired temperature, but it does not do so on the proper time scales and reflections were clearly evident. A total-system thermostat can be appropriate as a means of representing electron–phonon damping, i.e. absorption of mechanical energy into the electronic degrees of freedom [21]. However, in standard implementations, this heat is fully absorbed and is never transmitted back to the phonons in other regions of the material, and so such a method must be used with caution, physically motivated, and with physically appropriate coupling constants.

The coupled method employed here uses a quasistatic FEM. It is certainly feasible to use a fully dynamic FEM within, for instance, a lumped mass approximation. Such an approach has advantages and disadvantages, as noted previously, and is not more appropriate than the current method when dislocations exist in the continuum region. A hybrid version of the present method with a dynamic FEM model is also feasible. Specifically, in a dynamic FEM model, the pad atoms used to transmit deformation between the atoms and continuum could serve simultaneously as the stadium region by incorporating damping into the pad atom equations of motion. This would move the stadium region outside of the atomistic region, which is attractive. However, since the FEM constitutive behaviour is typically assumed to be linear (unless a quasicontinuum-type model is invoked), there can be a non-linear/linear mismatch at the interface that could lead to spurious reflections at the boundary. Different methods along these lines may be appropriate for different physical problems depending on, for instance, whether the loading is applied in the continuum or the atomistic region or on the temperatures of interest.

The present model with a damped stadium region in the atomistics is well suited to the full CADD model, wherein dislocations are detected in a 'detection band' lying within the atomistic region prior to reaching the atom/continuum boundary and then 'passed' as continuum entities in the continuum region [5]. In CADD, there thus already exists a region of atomistic material between the detection band and the boundary in which no significant non-linear deformations are permitted. In quasistatic simulations, this zone is $\sim$10 Å. So, implementation of stadium damping in a width of $\sim$20 Å will lead to only modified dynamics in the range of 10–20 Å from the atom/continuum boundary, where the atom damping is relatively low. The present model should thus provide good damping with little influence on the dynamics of the atomistic region of interest.

The present model is not the exact solution to the problem of dynamic, finite-temperature atomistic/continuum coupling. And, more elegant formal structures certainly exist for handling either dynamic problems at 0 K [8–12] or equilibrium problems at finite temperatures [2, 3]. One must keep in mind that such methods are not exact for non-linear deformations, may contain an adjustable parameter for temperature stability or may not handle non-equilibrium situations appropriately. Thus, as coupled methods such as CADD evolve to incorporate more physics at the mesoscale *outside* of the atomistic region, the need for efficient and accurate *approximate* methods competes with the desire for formal and exact results. We believe that the present model satisfies the need for a finite-temperature dynamic coupling method. Our future work will apply this model to study problems of complex deformation in mesoscale systems at finite temperatures such as crack growth, indentation deformation including cyclic loading, dislocation/grain-boundary interactions, nanotribology and nanofabrication simulations.

Acknowledgments

The authors gratefully acknowledge support from the US AFOSR through the MURI program 'Virtual Design and Testing: a Multiscale Approach' at Brown University, the NSF through the GOALI 'Nanoparticle Metrics for Computational Materials Mechanics' through the University of Minnesota and the NSF Materials Research Science and Engineering Center on 'Micro and Nano Mechanics of Materials' at Brown University.

The authors also acknowledge useful conversations with Professor M Marder, who has used the stadium method employed here for fully atomistic simulations, and thank the reviewers for useful comments and suggestions, particularly pointing our attention to [7].

References

[1] Curtin W A and Miller R 2003 *Modelling Simul. Mater. Sci. Eng.* **11** R33
[2] Curtarolo S and Ceder G 2002 *Phys. Rev. Lett.* **88** 255504
[3] Dupuy L, Miller R, Tadmor E B and Phillips R 2005 *Phys. Rev. Lett.* **95** 060202
[4] Holian B L and Ravelo R 1995 *Phys. Rev.* B **51** 11275
[5] Shilkrot L E, Miller R E and Curtin W A 2004 *J. Mech. Phys. Solids* **52** 755
[6] Evans D J and Holian B 1985 *J. Chem. Phys.* **83** 4069
[7] Holian B L, Voter A F and Ravelo R 1995 *Phys. Rev.* E **52** 2338
[8] Adelman S A and Doll J D 1974 *J. Chem. Phys.* **61** 4242
[9] Moseler M, Nordiek J and Haberland H 1997 *Phys. Rev.* B **56** 15439
[10] Cai W, de Koning M, Bulatov V V and Yip S 2000 *Phys. Rev. Lett.* **85** 3213
[11] Weinan E and Huang Z 2002 *J. Comput. Phys.* **182** 234
[12] Wagner G J and Liu W K 2003 *J. Comput. Phys.* **190** 249
[13] Abraham F F, Broughton J Q, Bernstein N and Kaxiras E 1998 *Europhys. Lett.* **44** 783
[14] Rudd R E and Broughton J Q 2000 *Phys. Status Solidi* b **217** 251
[15] Holland D and Marder M 1999 *Adv. Mater.* **11** 793
[16] Van der Giessen E and Needleman A 1995 *Modelling Simul. Mater. Sci. Eng.* **3** 689
[17] Landau L D and Lifshitz E M 1980 *Statistical Physics* Part 1 (New York: Pergamon) p 362
[18] Ercolessi F and Adams J B 1994 *Europhys. Lett.* **26** 583
[19] Allen M P and Tildesley D J 1997 Computer Simulation of Liquids (New York: Oxford University Press)
[20] Berendsen H J C, Postma J P M, Gunsteren W F, DiNola A and Haak J R 1984 *J. Chem. Phys.* **81** 3684
[21] Gumbsch P, Zhou S J and Holian B L 1997 *Phys. Rev.* B **55** 3445